Journal of Non-Crystalline Solids 356 (2010) 72–76

Contents lists available at ScienceDirect

Journal of Non-Crystalline Solids

journal homepage: www.elsevier.com/locate/jnoncrysol

Characterization of chemosynthetic Al_2O_3–$2SiO_2$ geopolymers

Xue-min Cui *, Le-ping Liu, Guang-jian Zheng, Rui-ping Wang, Jian-ping Lu

School of Chemistry and Chemical Engineering, Guangxi University, Nanning 530004, PR China

ARTICLE INFO

Article history:
Received 11 February 2009
Received in revised form 27 October 2009
Available online 1 December 2009

Keywords:
Diffraction and scattering measurements
Mass spectroscopy
SEM
Strength
Powders
Aluminosilicates
Polymers and organics
Sol–gel, aerogel and solution chemistry
Short-range order
X-ray diffraction

ABSTRACT

Pure chemosynthetic Al_2O_3–$2SiO_2$ geoploymers displaying positive alkali-activated polymerization properties and high compressive strength at room temperature were effectively fabricated utilizing a sol–gel method. The molecular structure of the precursor powder and resulting geopolymers were investigated by X-ray diffraction (XRD) and nuclear magnetic resonance (NMR) analysis. In addition, the mechanical and alkali-activated polymerization properties of these materials were also studied. NMR data revealed that the chemosynthetic powders began to contain 5-coordinated Al atoms when the calcination temperatures exceeded 200 °C. These calcined powders were capable of reacting with sodium silicate solutions at calcination temperatures exceeding 300 °C, which is, however, much lower than the temperature required to convert kaolin to Metakaolin.

1. Introduction

Due to their sinter-free, easy fabrication and low cost, aluminosilicate geopolymers are rapidly finding their way into numerous industrial applications such as in solid electrolytes, the immobilization of toxic, hazardous and radioactive wastes, advanced structural tooling and refractory ceramics, fire resistant composites used in the construction of buildings, aircraft, ships, race cars, etc., as well as the nuclear power industry. Aluminosilicate geopolymers represent one class of cross-linked, long-chain inorganic polymers who's three-dimensional structure consists of tetrahedral [AlO_4] and [SiO_4] units, resulting in excellent physical properties, among which are high strength, anti-corrosion, resistance to heat and long life [1,2].

At present, raw materials such as Kaolin clays, Metakaolin, fly ash and blast furnace slag are often used to create aluminosilicate geopolymers. However, the chemical composition of these materials is very complicated and a fundamental investigation into the mechanism of geopolymerization has proven to be difficult. Although Metakaolin is usually used in the study of geopolymerization mechanisms because of its simple chemical composition compared to the other common precursor materials, impurities in the Metakaolin complicate the study of the geopolymerization process [3–6]. Usually, Metakaolin is fabricated through calcination of Kaolin ($Al_2O_3{\cdot}2SiO_2{\cdot}2H_2O$) at 600–900 °C [7,8], however, the Metakaolin is not pure and the atomic ratio of Al/Si is not consistent due to the fact that the age and location of the Kaolin mines are different.

In order to overcome these disadvantages, the present investigation focuses on preparing pure Si–Al materials which then can be alkali-activated to form geopolymers. In earlier works, Hos et al. [5] subjected alumina and silica to 1555 °C as thus prepared a melt-quenched material as a precursor for the production of a geopolymer. Brew and MacKenzie [6] synthesized geopolymers utilizing fumed silica, a solution of sodium hydroxide and sodium aluminate. The current study also employs pure sources of Si and Al for producing geopolymers. In this study, a sol–gel method was developed for synthesizing and purifying Al_2O_3–$2SiO_2$ powders from tetraethoxysilane (TEOS) and aluminum nitrate nine-hydrate (ANN) as the starting materials [9]. However, the preparation process and analysis of the results yield differences from that reported in previous work. Specifically, in this study, pure Al_2O_3–$2SiO_2$ powders were prepared by a sol–gel method and alkali-activation tests of the powders were carried out. Furthermore, the structural characteristics of the powders and geopolymers were determined by XRD and MAS NMR, and the mechanical properties were reported as well.

2. Experimental procedures

Starting materials for the sol–gel synthesis are tetraethylorthosilicate (TEOS) and aluminum nitrate nonahydrate (ANN). Solvents

* Corresponding author.
E-mail address: cui-xm@tsinghua.edu.cn (X.-m. Cui).

0022-3093/$ - see front matter © 2009 Elsevier B.V. All rights reserved.
doi:10.1016/j.jnoncrysol.2009.10.008

for the synthesis are anhydrous ethanol and distilled water. Starting materials and solvents were mixed in the following molar ratios: Al_2O_3–SiO_2 was 1:2 and SiO_2–H_2O to EtOH was 1:18:12. In a typical synthesis, two solutions were prepared while stirring: Solution A, TEOS was dissolved in EtOH; and solution B, ANN was dissolved in a mixture of EtOH and distilled water. Solution B was then added slowly to solution A while stirring, and the resulting mixture was maintained at 70 °C until a gel formed. The gel was then dried at 105 °C. Finally, the dried gel powders were calcined in air at temperatures of 200 °C, 300 °C, 400 °C, 500 °C, 600 °C, 700 °C, 800 °C and 900 °C, respectively, for 2 h.

The physical properties of the dried gel powders and the calcined powders were investigated as follows: the particle size of chemosynthetic Al_2O_3–$2SiO_2$ powder was investigated by Zetasizer Nano S laser diffraction particle size analyzer. Because the particle size distribution was a range but not a point, hence, it's difficult to assign any reason for the repetitiveness error of Zetasizer Nano S laser diffraction particle size analyzer. The surface area was investigated by SSA-3600 intelligent specific surface tester. The repetitiveness error of SSA-3600 intelligent specific surface tester was about ±2%. The dried gel powder and the calcined powder was respectively added into NaOH solution at pH 11 ± 0.2 the mass ratios: the powder to NaOH solution was 1:20. The mixed liquid was stirred for 4 h, then was centrifugated by H1650 high speed bench centrifugal machine for 30 min at the speed of rotation 8000 r min^{-1}, at last the Al dissolution of up layer clear solution was investigated by EDTA titrate. The repetitiveness error of EDTA titrate was about ±1%.

A solution of sodium silicate (modulus, 2.8) and solid sodium hydroxide was mixed while stirring to produce an activator solution (modulus, 1.2), which reacted with the dried gel powders and calcined powders, respectively. Additional distilled water was added to adjust the water content of the mixture (the mass ratio of calcined powders to the solution of sodium silicate (modulus, 1.2) was 1:1). The geopolymeric paste was cast into 2.0 cm × 2.0 cm × 2.0 cm cubic molds and cured at room temperature for 72 h. The cubes were then removed from the mold and tested for compression strength using a XWW-20CE Universal Tester, and the repetitiveness error of the XWW-20CE Universal Tester was ±5%.

X-ray diffraction was recorded on an automated D/Max B X-ray diffractometer using Ni-filtered Cu Kα radiation with a scanning rate of 0.5° per min from 10° to 65° (2θ). An acceleration voltage of 40 kV and a current of 10 mA were applied.

^{29}Si and ^{27}Al NMR spectra were obtained on a Bruker AV300 NMR spectrometer with a 4 mm probe spin at 8 kHz for Al and 5 kHz for Si. The NMR conditions for ^{27}Al were 78.2 MHz resonance frequency, a 0.55 μs pulse width, a 1 s delay, referred to $Al(H_2O)_6^{3+}$; and for ^{29}Si were 59.6 MHz resonance frequency, a 1.9 μs pulse width, a 15 s delay, referred to tetramethylsilane (TMS).

3. Results

In this experiment, nanometer gel particles with a D_{50} of approximately 80 nm were obtained by a sol–gel method, however, this was improved to approximately 250 nm following calcination at 800 °C for 2 h. Compared with natural Metakaolin, the layered structure of the Al_2O_3 and SiO_2 within the synthetic powder was clearly not the same as in the Metakaolin, even after acidic leaching (immerged in 10 M sulphuric acid for 10 h). The reason for this is that the alumina, but not the silica, dissolves in sulphuric acid. SEM images are shown in Fig. 1(a) and (b). The experimental results indicate that the synthetic Al_2O_3–$2SiO_2$ powders also have an irregular layered structure, which is different from that of natural Metakaolin, with an individual layer likely composed of many particle clusters, as shown in Fig. 1(b).

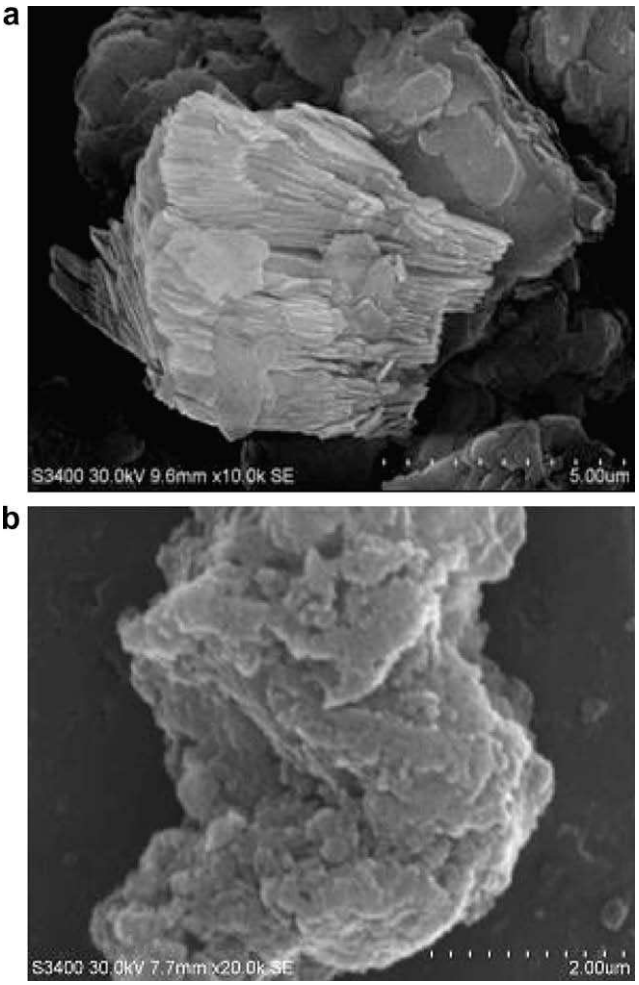

Fig. 1. SEM photo of erosional powders in 10 mol L^{-1} sulphuric acid for 10 h: (a) natural Metakaolin, and (b) synthetic Al_2O_3–$2SiO_2$ powder.

The results of the compressive strength of synthetic Al_2O_3–$2SiO_2$ geopolymers are presented in Table 1. These data indicate that the harden geopolymeric sample produced from powder calcined at 200 °C had no strength, while maximum strength was obtained when the precursor material was calcined at temperatures in the range of 700–800 °C. However, when calcination temperatures exceeded 800 °C, the compressive strength of the geopolymer was lost.

This effect of precursor calcination temperature on the strength of the geopolymer is similar to what is observed with Metakaolin [7,8]. A more detailed observation, however, reveals that calcined powders begin to manifest effects at 300 °C, while in the case of Metakaolin, the effects usually appear at about 500 °C. This observation suggests that Al_2O_3–$2SiO_2$ geopolymers produced from chemosynthetic Al_2O_3–$2SiO_2$ powders might possibly be prepared at lower temperatures than Metakaolin geopolymers. Such a lower temperature effect might allow for the addition of property-enhancing additives that otherwise would be unstable at the high temperatures required to prepare Metakaolin geopolymers.

Table 2 presents a comparison between the physical properties of the dried gel powders and the calcined powders. Clearly, the calcination process aggrandizes the surface area of synthetic Al_2O_3–$2SiO_2$ powders, however, the Al dissolution in NaOH at pH 11 ± 0.2 is slightly greater than for the dried gel powders, 8.66 ± 0.09% vs. 6.04 ± 0.06%, respectively. Based on the data in Table 1, the Al dissolution in NaOH does not represent geopolymerization activity.

Table 1
Compressive strength of the samples synthesized from dried gel powders or calcined powders.

Starting material for samples	Dried gel powders	Calcined powders							
Calcined temperatures (°C)	105	200	300	400	500	600	700	800	900
Compressive strength of geopolymer material after casting for 72 h (MPa)	0	0	4.7 ± 0.2	4.8 ± 0.2	4.8 ± 0.2	14.2 ± 0.7	28.3 ± 1.4	28.2 ± 1.4	0

Table 2
Comparison of the physical properties between dried gel powders and calcined powders.

	Chemical composition (Si/Al)	Particle size D_{50} (nm)	Surface area (m^2/g)	Al dissolution in NaOH for 4 h (%)@pH 11 ± 0.2
Dried gel powders	1:1	50	669.27 ± 13.39	6.04 ± 0.06
Powders calcined at 800 °C for 2 h	1:1	250	321.58 ± 6.43	8.66 ± 0.09

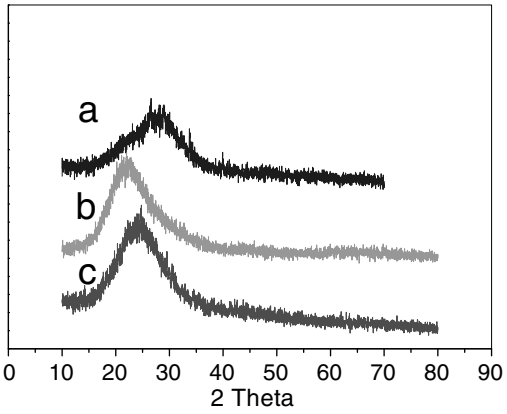

Fig. 2. XRD patterns of (a) geopolymeric material; (b) calcined powder at 800 °C for 2 h; and (c) dried gel powder at 105 °C.

The XRD patterns of powders calcined at different temperatures are similar, with all samples showing a broad diffusion peak corresponding to a diffraction angle between 15° and 40°. The typical XRD patterns of Al_2O_3–$2SiO_2$ dried gels, calcined powders and geopolymeric materials are shown in Fig. 2. The center of the diffraction peak produced from the 800 °C-calcined powder is at lower angle than that of the dried gel. The size of the diffraction angle reflects the change in spacing between the aluminosilicate layers [5]. Thus, after calcination, the short range molecular structure of Al_2O_3–$2SiO_2$ should be more ordered than that in the non-calcined sample. The degree of polycondensation of the synthesized powders was verified by the reaction between calcined or dried gel Al_2O_3–$2SiO_2$ powders and $Na_2O{\cdot}xSiO_2$ (x is 1.2 here) in aqueous solutions at room temperature. The experimental results indicate that dried gel powders lack polycondensation activity, while in contrast, the calcined powders exhibit good alkali polycondensation activity. Thus, geopolymers can be synthesized from calcined powders and aqueous alkali silicate at room temperature. Based on the experimental results, the inter-layer spacing of the aluminosilicate molecules may be the key factor in defining the microstructure, which can be characterized by solid state NMR.

Fig. 3 shows the TG–DTA curves of the dried gel in air. At a temperature of 1005.8 °C, an exothermic peak appeared on the DTA curve representing the formation of a crystalline phase. The analysis of that crystalline phase will be studied later.

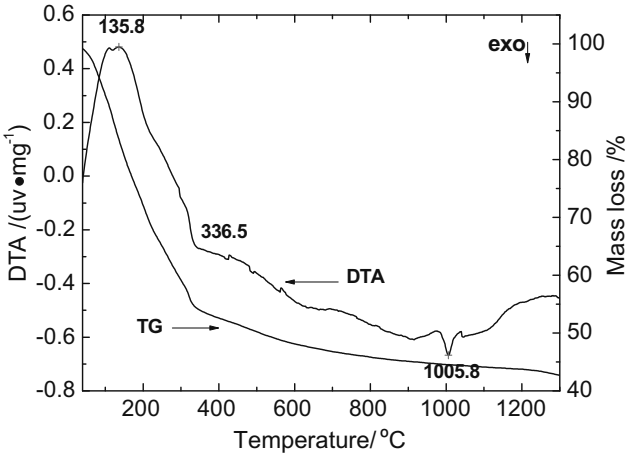

Fig. 3. TG–DTA curves of the dried gel in air.

4. Discussions

In this work, the compressive strength data have been collected from three samples at least. The compressive strength of geopolymer is some degree of uncertainty because of instrument factors and experimental samples, but we try to make the experimental errors to the lowest or smallest, such as measuring at the same time, many measuring samples, and so on. If the measuring errors are not over 10%, we think the changing tendency is to be trusted.

The ^{27}Al spectrum is generally considered the key factor in characterizing alkali-activated polymerization. Here, the ^{27}Al MAS NMR spectra of the dried gel and calcined powders are shown in Fig. 4. The spectrum of the dried gel consists of a single peak centered at approximately 1 ppm and assigned to 6-coordinated Al [Al(VI)], indicating that the Al environment of the dried gel is similar to that of kaolinite [8,9]. With increasing temperature, the calcined powders exhibit two new resonance peaks, one at approximately 55 ppm, attributable to 4-coordinated Al [Al(IV)] and one at approximately 25 ppm due to 5-coordinated Al [Al(V)]. The Al coordination changes of the powders are in agreement with those of dehydroxylated kaolinite [8,9]. In particular, it should be noted that the peaks related to Al(IV) and Al(V) appeared in the spectra of the powders calcined at 200 °C and 300 °C, while similar peaks usually appeared in kaolinite at temperatures over 480 °C. Rocha and Klinowski [10] believed that Al(V) was the principal indicator of the reactivity of the material and characterized a transitional state. The presence of Al(V) may explain why the dried gel calcined at 300 °C began to show some property of alkali-activation (see Table 1). In addition, the peaks attributed to Al(V) are strengthened as the temperature increases and this apparent increase in Al(V) corresponds to the increase in compressive strength, indicating that Al(V) may be directly involved (see Table 1 and Fig. 4), as originally suggested by Rocha and Klinowski [10].

The ^{29}Si spectra of the dried gel and calcined powders are shown in Fig. 5. The principal features of the ^{29}Si spectrum of the dried gel are the two peaks at approximately −103 ppm and −106 ppm, while the ^{29}Si spectrum of the calcined powder treated

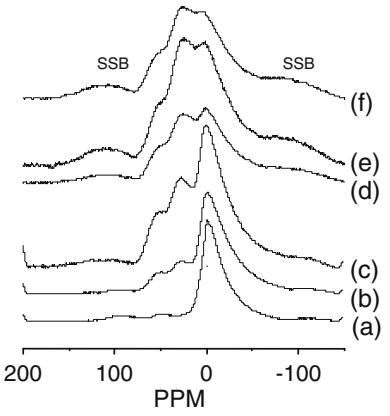

Fig. 4. ^{27}Al MAS NMR spectra of the dried gel at 105 °C (a) and powders calcined at various temperatures (SSB stands for spinning sidebands): (b) 200 °C; (c) 300 °C; (d) 600 °C; (e) 800 °C; and (f) 900 °C.

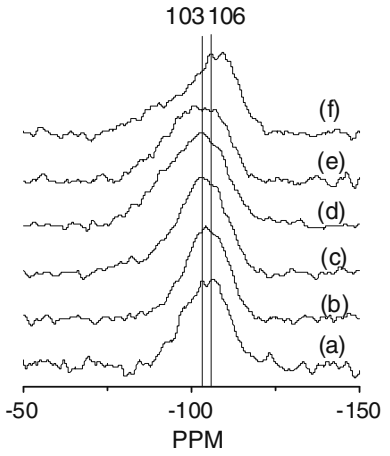

Fig. 5. ^{29}Si MAS NMR spectra of the dried gel at 105 °C (a) and powders calcined at various calcination temperatures: (b) 200 °C; (c) 300 °C; (d) 600 °C; (e) 800 °C; and (f) 900 °C.

at 200 °C contains a peak at approximately −104 ppm with two shoulders at around −103 ppm and −106 ppm. From the other ^{29}Si spectra shown in Fig. 5, we speculate that the peak at about −104 ppm for the calcined powders at 200 °C [spectrum (b)] may actually be an artifact resulting from the superposition of signals peaking at −103 and −106 ppm, which can be resolved in the other spectra. Framery and Mutin [11] have presented ^{29}Si MAS NMR spectra of an acid-catalyzed xerogel obtained from hydrolysis of tetraethoxysilane (TEOS) in ethanol without an Al source. Interestingly, the spectra indicated the presence of Q3 (−101 ppm) and Q4 (−110 ppm) sites in a ratio of roughly 1:1. Since the replacement of one silicon with one aluminum at a given site caused a downfield shift of approximately 5 ppm [14], the signal of −106 ppm in this study could be assigned to Q4 (1Al), while the signal at −103 ppm might be attributed to Q3, since the resonance peak of Si in Metakaolin is about −103 ppm [12,13]. Therefore, we see that data from XRD and ^{27}Al MAS NMR analysis all contain evidence of structural similarities between the powders calcined at 300–800 °C and Metakaolin.

Fig. 5 also indicates that the FWHMs (full-width-at-half maximum) of the spectra of the powders calcined at 200 °C and 300 °C are approximately the same, about 16 ppm, which is far greater than that of kaolinite (about 2.5 ppm), and yet slightly less than that of Metakaolin (about 20 ppm) [8,9]. Therefore, these

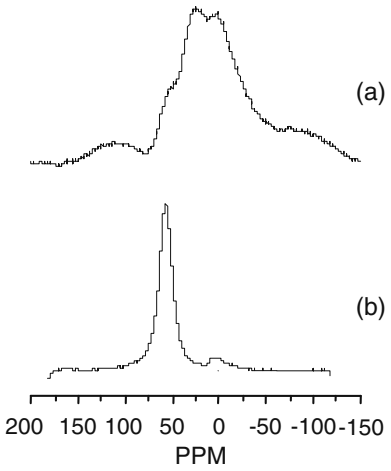

Fig. 6. ^{27}Al MAS NMR spectra of (a) the powder calcined at 800 °C and (b) its subsequent alkali-activated sample.

calcined powders possessed many of the characteristics of Metakaolin, such as an amorphous XRD pattern, the presence of Al(V) in Al NMR spectra, and the location and FWHMs of Si NMR spectra. In the study presented here, 200 °C-calcined powder was also amorphous, contained some Al(V), and began to display properties of alkali-activation in sodium silicate solutions. However, it demonstrated no compressive strength whatsoever, and therefore needs to be studied further.

With an increase in calcination temperatures up to 600 °C, the ^{29}Si spectrum of the samples still displays a peak at approximately −103 ppm and a shoulder at about −106 ppm. In addition, the center of gravity of the signal shifted downfield and the FWHM moved from about 16 ppm to 22 ppm. At 800 °C, the center of gravity of the signal remained shifted downfield, and a new peak appeared at approximately −101 ppm, possibly due to Q4 (2Al). With a change in temperature from 800 °C to 900 °C, the center of gravity of the spectrum shifted back to the higher magnetic field, with a peak at about −106 ppm and another peak at around −109 ppm, assigned to Q4 (0Al) and related to the presence of amorphous SiO_2 or cristobalite [8,9]. Since the maximum of each of the two peaks is nearly the same, it is possible they represent a single peak and if so the FWHM of the spectrum would be approximately 16 ppm (less than that at 800 °C). While the rationale presented here is not definitive, there is evidence that the environment of the Si atoms changes to a more ordered state (the formation of some crystalline phases) when the calcination temperature was shifted from 800 °C to 900 °C. Similar results appeared when kaolinite was calcined at about 850–900 °C [8,9]. Maybe this formation of some crystalline phases resulted in the powders not to display the alkali-activation property when treated above 900 °C.

The ^{27}Al MAS NMR spectra of the powder calcined at 800 °C and the subsequent alkali-activated sample are presented in Fig. 6. It appears that during the reaction, Al(V) and Al(VI) were converted to tetrahedral Al(IV) sites and as a result the broad spectrum was sharpened into a well-defined peak, which is a typical characteristic of geopolymers [12].

The ^{29}Si MAS NMR spectra of the powder calcined at 800 °C and its alkali-activated sample are presented in Fig. 7. The center of gravity of the signal was at about −102 ppm before the reaction, and then shifted to the typical geopolymer position of −92 ppm following the reaction. Previous studies show that ^{29}Si MAS NMR spectrum of fully cured geopolymers reveals a broad resonance peak located at approximatley −85 to −95 ppm depending on the Si/Al ratio [12,14,15]. In summary, the change in the ^{29}Si MAS NMR spectra of samples before and after the reaction also

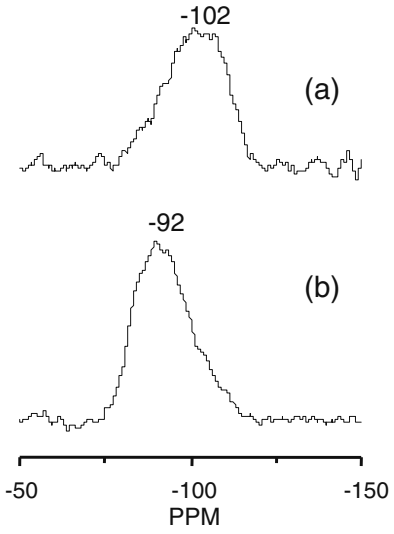

Fig. 7. ^{29}Si MAS NMR spectra of (a) the powder calcined at 800 °C and (b) its subsequent alkali-activated sample.

demonstrates the characteristics of geopolymerization, and in fact the spectra are similar to those of Metakaolin and its alkali-activated product.

Pure Al_2O_3–$2SiO_2$ precursors (powders) for a geopolymeric material have been prepared by a simple sol–gel method. The alkali-activated products derived from these precursors meet the general criteria for a geopolymer. Since the purity and Si/Al ratio of the precursors for the geopolymer are easily adjusted in the sol–gel process, the properties and composition of the precursors can be controlled with relative ease. Hence, these precursors and the geopolymers resulting from them need to be investigated further in order to fully understand their wide ranging potential applications.

5. Conclusions

Pure chemosynthetic Al_2O_3–$2SiO_2$ geoploymers displaying positive alkali-activated polymerization properties and high compressive strength at room temperature were effectively fabricated utilizing a sol–gel method. The molecular structure of the precursor powder and resulting geopolymers were investigated by X-ray diffraction (XRD) and nuclear magnetic resonance (NMR) analysis. In addition, the mechanical and alkali-activated polymerization properties of these materials were also studied.

The results indicate that the reactivity of the chemosynthetic Al_2O_3–$2SiO_2$ powder was best when calcinated at temperatures from 300 °C to 800 °C, with the highest reactivity occurring in the powder calcined at 800 °C. For powder calcined below 300 °C or above 800 °C, no reactivity was observed due to the disappearance of Al(V). Therefore, the Al(V) might be directly involved in compressive strength as compressive strength was zero for precursors calcined below 300 °C or above 800 °C.

From NMR and XRD analyses, it can be shown that the microstructure of powders calcined at 300–500 °C is different from that of Metakaolin. For example, the powders start to become alkali-activated at a calcination temperature of 300 °C which is far lower than the temperature at which kaolin begins the transformation to Metakaolin.

Acknowledgments

This work was supported by Chinese Natural and Science Fund (Grant Nos.: 50962002 and 50602006) and Program for Excellent Talents in Guangxi Higher Education Institutions (Grant No.: RC2007003).

References

[1] P. Duxson, A. Ferna′ndez-Jime′nez, J.L. Provis, G.C. Lukey, A. Palomo, J.S.J. Van Deventer, J. Mater. Sci. 42 (2007) 2917.
[2] X.M. Cui, G.J. Zheng, Y.C. Han, et al., J. Power Sources 184 (2008) 652.
[3] C.K. Yip, G.C. Lukey, J.L. Provis, J.S.J. Van Deventer, Cement Concrete Res. 38 (2008) 554.
[4] H. Rahier, J. Wastiels, M. Biesemans, R. Willlem, G. Van Assche, B. Van Mele, J. Mater. Sci. 42 (2007) 2982.
[5] J.P. Hos, P.G. McCormick, L.T. Byrne, J. Mater. Sci. 37 (2002) 2311.
[6] D.R.M. Brew, K.J.D. MacKenzie, J. Mater. Sci. 42 (2007) 3990.
[7] P. De Silva, K. Sagoe-Crenstil, V. Sirivivatnanon, Cement Concrete Res. 37 (2007) 512.
[8] J.L. Provis, G.C. Lukey, J. Deventer, Chem. Mater. 17 (2005) 3075.
[9] J. Rocha, J. Klinowski, Phys. Chem. Miner. 17 (1990) 179.
[10] J. Rocha, J. Klinowski, Angew. Chem. Int. End. Eng. 29 (1990) 553.
[11] E. Framery, P.H. Mutin, J. Sol–Gel Sci. Technol. 24 (2002) 191.
[12] P.S. Singh, T. Bastow, M. Trigg, J. Mater. Sci. 40 (2005) 3951.
[13] L. Weng, K. Sagoe-Crentsil, J. Mater. Sci. 42 (2007) 2997.
[14] P. Duxson, J.L. Provis, G.C. Lukey, F. Separovic, J.S.J. Van Deventer, Langmuir 21 (2005) 3028.
[15] R.A. Fletcher, K.J.D. MacKenzie, C.L. Nicholson, S. Shimada, J. Eur. Ceram. Soc. 25 (2005) 1471.

Available online at www.sciencedirect.com
SCIENCE DIRECT®
Journal of Solid State Chemistry 174 (2003) 482–488
JOURNAL OF SOLID STATE CHEMISTRY
http://elsevier.com/locate/jssc

Effect of the Al/Si atomic ratio on surface and structural properties of sol–gel prepared aluminosilicates

V. La Parola,[a] G. Deganello,[a,b] S. Scirè,[c] and A.M. Venezia[b,*]

[a] *Dipartimento di Chimica Inorganica e di Chimica Analitica "Stanislao Cannizzaro" Università di Palermo, Viale delle Scienze, Parco D'Orleans 90128, Palermo, Italy*

[b] *Istituto per lo Studio dei Materiali Nanostrutturati, ISMN-CNR Sezione di Palermo, Via Ugo La Malfa 153, 90146, Palermo, Italy*

[c] *Dipartimento di Scienze Chimiche, Università di Catania, Catania, Viale A. Doria 6, 95125, Italy*

Received 20 December 2002; received in revised form 28 May 2003; accepted 30 May 2003

Abstract

A series of aluminosilicates with an Al/Si ratio ranging from 0 to ∞ (0 for pure silica and ∞ for pure alumina) was prepared by sol–gel process and characterized by surface and structure techniques. Aluminum tri*sec*butoxide and tetramethylorthosilicate were used as precursors for the sol–gel synthesis. The acidic properties of the oxides were studied by determination of the zero point charges, through mass titration method, and, for selected samples, by FT-IR spectroscopy of adsorbed pyridine used as a probe for both Brønsted and Lewis acidity. A dependence of the acidity on the Al/Si atomic ratio was found. According to the X-ray diffraction patterns, all the oxides have an amorphous structure except pure alumina exhibiting a γ-alumina pattern. The surface areas of the mixed oxides increase with increasing amount of alumina and are higher as compared to the individual oxides. The surface elemental distribution and electronic properties were investigated by X-ray photoelectron spectroscopy. According to the results, good agreement between the surface Al/Si atomic ratio and the analytical ratio is obtained.

Keywords: Silica-aluminas; Brønsted and Lewis acid; XPS; IR spectroscopy

1. Introduction

The availability of suitable supports for metal catalysts is of fundamental importance in heterogeneous catalysis. Due to its good textural and mechanical properties and its low cost, γ-alumina is one of the most used supports, especially in hydrotreating catalysis [1]. The chemical interaction between alumina and supported phases may contribute to the catalyst stability against sintering processes. Amorphous silica with its generally high surface area and high purity is also used as support [2]. However it generally leads to lower activity catalysts, and since it interacts less with the active species, allows detailed studies of catalysts characterization [3]. Mixed oxides such as amorphous silica aluminas (ASA) possess interesting properties especially when they are well mixed on a molecular scale. The combination of the two oxides may give rise to surface acid sites which are not present in either of the pure components [4]. The maximum acid strength of some mixed oxides was found to correlate with the average electronegativity of the cations [4–5]. Several models have been proposed to explain the appearance of the acid sites in a mixed oxide [6]. Following certain rules, once the excess of charge near the cation is calculated it follows that a positive charge is associated with Lewis acid sites, whereas excess negative charge is associated with Brønsted sites [5]. The surface acidity of the mixed oxides depends on the Al/Si atomic ratio [7]. The sol–gel chemistry allows to prepare mixed silica-alumina oxides with different Al/Si ratio and with well-defined surface areas, pore distribution and crystallinity [8]. However the attainment of a good molecular scale mixing is still a hard task [9]. The characteristics of the obtained oxides strongly depend on the sol–gel parameters such as the precursor molecules, their concentration, the solvent, the temperature, the amount of water of hydrolysis, and the pH [3–4]. Regarding the use of amorphous silica-aluminas as supports for

*Corresponding author. Fax: +390-916-809-399.
E-mail address: anna@pa.ismn.cnr.it (A.M. Venezia).

0022-4596/03/$ - see front matter © 2003 Elsevier Inc. All rights reserved.
doi:10.1016/S0022-4596(03)00321-9

hydrotreating catalysts [10–11], a dependence of the catalytic activity of the supported CoMo catalysts on the alumina/silica ratio and on the related acid–base properties was found [12]. Moreover the opposite effect of sodium ions added to pure silica and to a commercial amorphous aluminosilicate, on the hydrodesulfurization activity of CoMo catalysts, lead us to prepare in a controlled way a series of aluminosilicates with an Al/Si ratio ranging from 0 to ∞ (0 for pure silica and ∞ for pure alumina) in order to investigate in details the support effect in relation to its acidity and structural properties [10–13]. To this aim a series of aluminosilicates was prepared by sol–gel route and characterized by several techniques. The acidic properties of the oxides were studied by determination of the zero point charges (ZPC), through mass titration method, and, for selected samples, by IR spectroscopy of adsorbed pyridine used as a probe for both Brønsted and Lewis acidity. The surface and structural properties were studied by X-ray photoelectron spectroscopy and X-ray diffraction analyses. The morphology, in terms of surface areas, pore distribution and pore volume, was studied by N_2 physisorption.

2. Experimental

2.1. Preparation of the oxides by the sol–gel

All operations were performed under an atmosphere of pure argon. All chemicals (Aldrich Chemical Company Inc.) were of reagent grade purity and used as received. The required amounts of $Al(O\text{-}sec\text{-}Bu)_3$ and $Si(OEt)_4$ were mixed together. The solution was stirred for 3 h at room temperature under Ar flow in order to obtain a homogeneous mixture. The temperature was then raised to 353 K and the hydrolysis was performed by adding water (pH = 9 for ammonia) in stoichiometric amount to the rapidly stirred reaction mixture to allow the slow hydrolysis of the two alkoxides [4]. The hydrolysis in a basic environment should indeed promote formation of a mesoporous structure with less initial surface area as compared to samples prepared with acid hydrolysis, but more stable during heat treatment [4]. The gel, which formed in a few minutes, was left for 5 h under reflux and constant stirring. Then it was aged in air inside the flask for 5 days at room temperature. The colorless gel, homogeneous at visual inspection, was washed with sec butanol to remove possible traces of unhydrolyzed alkoxide. The washing fractions were completely clear on water addition. The xerogels were calcined in air at 773 K overnight. The list of prepared supports is given in Table 1. The nominal Al/Si atomic ratio corresponded to the bulk ratio as confirmed from the X-ray fluorescence analyses. In order to check the reproducibility of the preparation method, the syntheses of supports with the same Al/Si ratios were repeated at least twice.

Table 1
Al/Si bulk (nominal) and XPS derived atomic ratios, surface areas and zero point charges. In parentheses the atomic ratios obtained considering only the Si 2*p* component at high energy are reported

Samples	$Al/Si_{(bulk)}$	$Al/Si_{(XPS)}$	S (m^2/g)	Z.P.C
*s*AlO	∞	∞	210	n.d.
*s*3	3.50	2.46 (3.23)	480	6.4
*s*2	2.34	1.85 (2.28)	488	5.6
*s*1	1.18	1.11 (1.22)	450	4.5
*s*0.3	0.39	0.30 (0.31)	355	4.1
*s*0.17	0.18	0.11	150	3.7
*s*0	0	0	143	5.2

2.2. Catalyst characterization

2.2.1. Zero point charge

The zero point charge of the supports was determined by mass titration [14]. According to this method, the variation of pH of a water solution containing increasing amount of solid was monitored until the steady state value of pH (ZPC) was reached.

2.2.2. IR spectroscopy

IR spectra were recorded with a Perkin Elmer System 2000 FT-IR spectrophotometer with a resolution of $2\,cm^{-1}$. The powdered samples were compressed into thin self-supporting discs of about $25\,mg\,cm^{-2}$ and 0.1 mm thick. The disc was placed in an IR cell which allows thermal treatments in vacuum or in a controlled atmosphere. In the cell all samples were evacuated at 400°C for 1 h and finally cooled at room temperature. Pyridine was then admitted by opening for some seconds the valve of the vessel containing the substance at 283 K. Subsequent evacuations were then performed at 423 K. Data are reported as difference spectra obtained by subtracting the spectrum of the sample before the admission of pyridine and are normalized to the same amount of catalysts per cm^2.

2.2.3. X-ray diffraction

X-ray diffraction measurements for the structure determination were carried out with a Philips vertical goniometer using Ni-filtered Cu$K\alpha$ radiation. A proportional counter and 0.05° step sizes in 2θ were used.

2.2.4. BET analyses

The microstructural characterization was performed with a Carlo Erba Sorptomat 1900 instrument. The fully computerized analysis of the adsorption isotherm of nitrogen at liquid nitrogen temperature, allowed obtaining, through the BET approach, the specific surface area of the samples. By analysis of the desorption curve,

using the Dollimore and Heal calculation method, the pore size volume distribution was also obtained [15].

2.2.5. XPS

The X-ray photoelectron spectroscopy analyses were performed with a VG Microtech ESCA 3000 Multilab, equipped with a dual Mg/Al anode. The spectra were excited by the non-monochromatized Al$K\alpha$ source (1486.6 eV) run at 14 kV and 15 mA. The analyzer operated in the constant analyzer energy (CAE) mode. For the individual peak energy regions, a pass energy of 20 eV set across the hemispheres was used. Survey spectra were measured at 50 eV pass energy. The sample powders were analyzed as pellets, mounted on a double-sided adhesive tape. The pressure in the analysis chamber was in the range of 10^{-8} Torr during data collection. The constant charging of the samples was removed by referencing all the energies to the C 1*s* set at 285.1 eV, arising from the adventitious carbon. The invariance of the peak shapes and widths at the beginning and at the end of the analyses ensured absence of differential charging. Analyses of the peaks were performed with the software provided by VG, based on non-linear least-squares fitting program using a properly weighted sum of Lorentzian and Gaussian component curves after background subtraction according to Shirley and Sherwood [16–17]. Atomic concentrations were calculated from integral intensity of the chosen peaks using ionization cross sections provided by the instrument software. The binding energy (BE) values are quoted with a precision of ± 0.15 eV.

2.3. Results and discussion

The oxides with different Al/Si overall ratios are listed in Table 1 along with the surface ratios as found by XPS, the surface area and the zero point charge. The ZPC or IEPS (isoelectric point) is an important property in the design of oxide supported catalysts since it determines the adsorption features of the different oxides as function of the pH of the impregnating solution [18]. The ZPC is a measure of the polarizability of the material which tends to be surface charged once suspended in aqueous solution. The surface charge, being neutralized by adsorption of OH^- or H^+ is a measurements of the total surface acidity of the solid. As can be observed in the table, the ZPC increases with the increase of the amount of alumina in the mixed oxides. The ZPC value of sol–gel prepared silica is higher as compared to the values in Ref. [18]. Differences are likely to be due to the preparation method and to the presence of structural defects.

Oxide surfaces exhibit both Brønsted and Lewis acidity. The Brønsted acid sites arise from silanol groups which can be generated when a trivalent cation, like Al^{3+}, is present in tetrahedral coordination with oxygen. When the oxygen anions are shared between the cations, net negative charges are created on aluminum and are compensated by protons giving rise to terminal silanol groups and to the more acidic bridging hydroxyl groups. The Lewis acidity arises from partly uncoordinated metal cations and anions present at the surface of metal oxides which with water (always present in the environment) produce surface hydroxy-groups [19]. They are also formed through the isomorphous substitution of Si^{4+} lattice sites by Al^{3+} ions. In pure silica, characterized by covalent Si–O bonding, Brønsted acidity is low and Lewis sites are absent unless silica has been activated at very high temperatures [19–20]. A study of the surface acidity may be done by using a basic molecule, such as pyridine, as a probe which interacts through the electronic lone pair of its N atom with sites of different acidity and is able to probe both Lewis and Brønsted acidity [21]. This interaction is studied by IR spectroscopy. The stretching vibrations $\nu_{8a,b}$ and $\nu_{19a,b}$ of the pyridine ring are the most sensitive modes used in IR studies to evaluate the strength of the adsorptive interaction. Generally the bands at ca. 1640 and 1540 cm^{-1} are characteristics of pyridinium ions (adsorption of pyridine on Brønsted sites), whereas bands in the region 1600–1630 cm^{-1} and 1440–1455 cm^{-1}, are attributed to coordinately adsorbed pyridine on Lewis sites [19]. The band at 1492 cm^{-1} is less informative, being associated with both Brønsted and Lewis site. While the frequencies of the bands of pyridinium do not change substantially upon varying the acidity of the solid, the bands related to coordinatively bound pyridine move to high frequency as the strength of interaction increases, the ν_{8a} band being more sensitive. In Fig. 1a the FT-IR spectra in the region 1700–1400 cm^{-1} over three silica-alumina samples, after admission of pyridine and subsequent evacuation at 423 K to eliminate the physisorbed pyridine, are shown. The *s*3 sample exhibits a spectrum which is typical of the adsorption of pyridine on Lewis acid sites. The main features of the spectrum are the ν_{19b} band at 1452 cm^{-1} and the ν_{8a} band at 1625 cm^{-1}. Very weak bands at ca. 1540 and 1640 cm^{-1} can be also noted, indicating the presence of a very low amount of Brønsted acid sites on the catalytic surface of this sample. Therefore it is evident from the figure that the *s*3 sample has considerable Lewis but very low Brønsted acidity. On *s*03 and *s*1 samples the peaks characteristics of pyridinium ions are more intense, clearly indicating that the two samples present a higher Brønsted acidity compared to that of the alumina rich sample *s*3. The intensity ratio between the peak at 1640 cm^{-1} and the one at 1625 cm^{-1} seems to indicate that in *s*0.3 the ratio of the Brønsted sites to Lewis sites is larger than in *s*1. As indicated by the invariance of the peak positions among the three considered samples, the acid sites have similar strength. Based on the results, concerning the

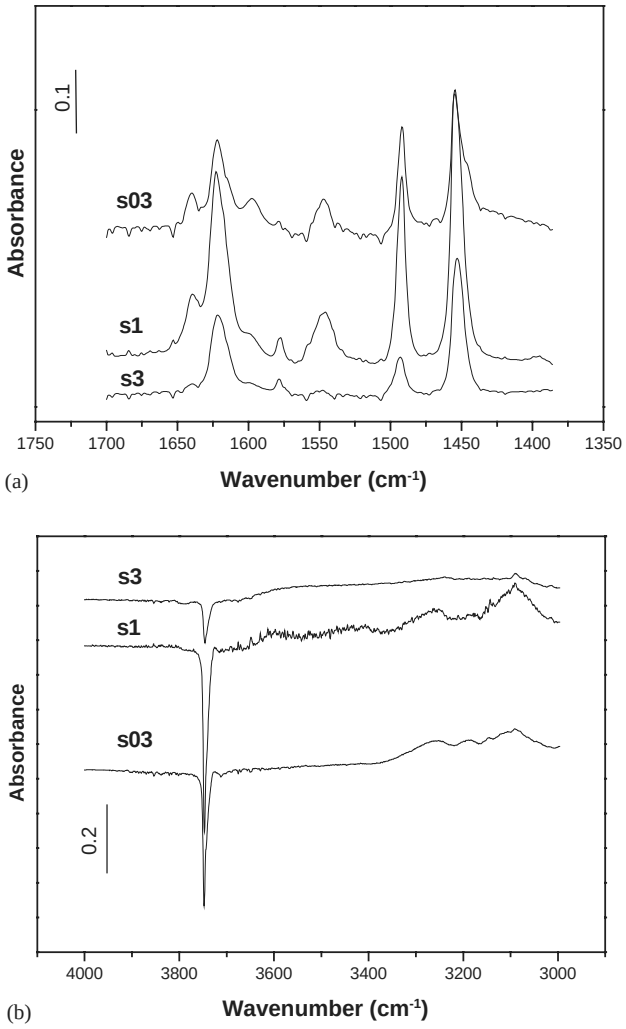

Fig. 1. FT-IR spectra of selected silica-alumina samples after admission of pyridine and subsequent outgassing at 423 K. Data are reported as difference spectra obtained by subtracting the spectrum of the sample before the admission of pyridine.

Lewis/Brønsted acidity ratio, the following order $s3 > s1 > s03$ is obtained. Such acidity order is in accord with the rules formulated by Tanabe [5–6]. Following these rules, the excess of positive charge, calculated for the aluminum rich oxides, is associated with Lewis acid sites whereas the excess of negative charge in the silica enriched oxides, is associated with Brønsted sites [6]. In Fig. 1b, in which the FT-IR spectra in the region 4000–3000 cm^{-1} after admission of pyridine and subsequent evacuation at 423 K are shown, it is possible to observe that pyridine adsorption brings about the decrease of the OH stretching band at 3746 cm^{-1} (strong negative peak), characteristic of the silanol band observed in pure silica [22]. However at a careful inspection of the band, an asymmetry at lower frequency (3742 cm^{-1}) is observed. In accord with literature [23] this feature may be attributed to the more acidic bridging hydroxyl groups able to form the pyridinium ion, as detected in Fig. 1a. There is no evidence of alumina-like hydroxyl bands.

For all the analyzed samples, the N_2 adsorption curves in the low-pressure region conformed to the BET Type II isotherm, whereas in the higher-pressure region the hysteresis loop typical of mesoporous materials appeared. The specific surface areas obtained from the BET method are listed in Table 1. The areas of the mixed oxides are larger as compared to the single oxides. Moreover the surface area decreases with the increase of silica amount. This result differs from the one obtained for mixed alumina-silica oxides prepared by sol–gel, using different precursors and different preparation steps [24]. In that case a decrease of the surface area with increase of alumina content was found [24]. In Fig. 2 the pore distributions of the silica-alumina oxides are shown. All of the samples have mesopores. The oxides with high alumina content, like *s*AlO, *s*3 and *s*2, exhibit a pore distribution centered at the low size end of the mesopore region, the mixed oxides with high silica content, *s*0.3 and *s*0.17, have larger pores. As mentioned in the experimental part, sol hydrolysis in basic environment may have promoted formation of mesoporous structure [4].

The X-ray diffractograms of the mixed oxides after calcinations at 773 K are shown in Fig. 3. Pure silica and pure alumina show features typical of amorphous silica and of γ-alumina with contribution from a distorted θ-alumina respectively, while all the other diffractograms are typical of amorphous aluminosilicates. The amorphism of the obtained silica-alumina systems is generally indicative of a well-mixed two component oxide [25].

The XPS survey spectra of the samples evidenced only oxygen, silicon, aluminum and carbon peaks. The binding energy of Al 2*p*, Si 2*p* and O 1*s* peaks with the relative full-width at half-maximum (FWHM) are summarized in Table 2. Silicon and oxygen are strongly affected by the presence of aluminum; the binding energy of these peaks decreases with increasing aluminum content and for all samples the difference between the two energies, Δ[O(1*s*)–Si(2*p*)], considering the high energy Si 2*p* component, is equal to 429 eV. As reported

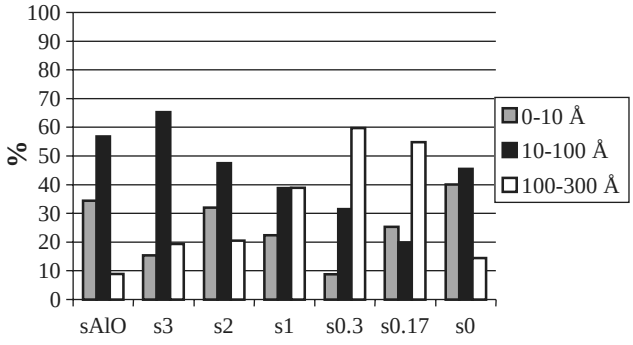

Fig. 2. Pore distribution of the silica-alumina oxides.

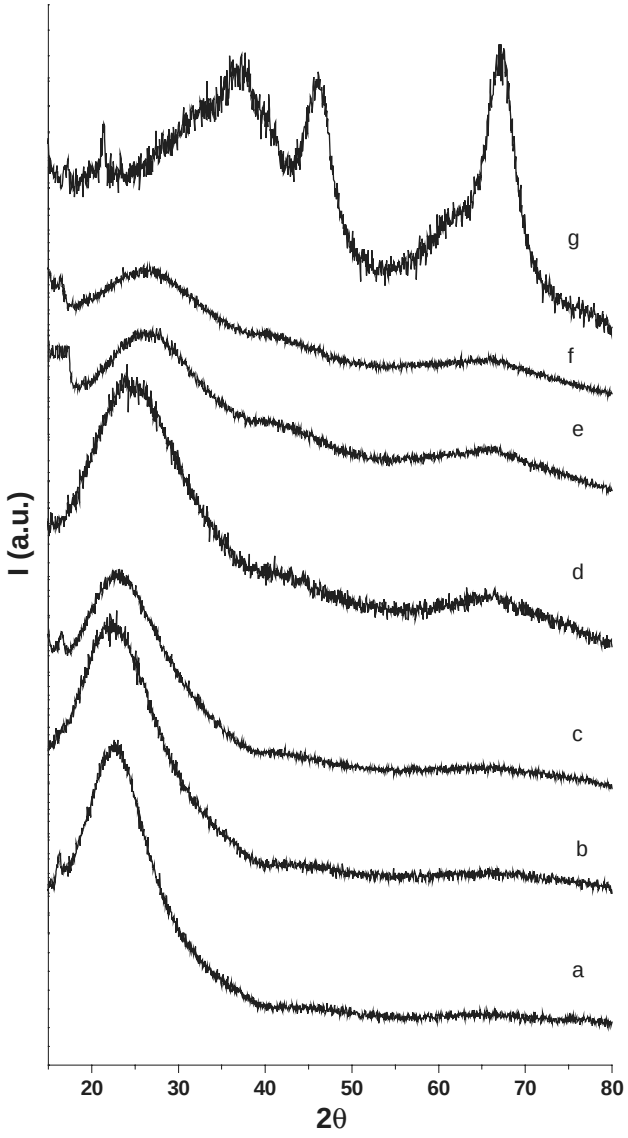

Fig. 3. X-ray diffractograms of the oxides. (a) *s*0, (b) *s*0.17, (c) *s*0.3, (d) *s*1, (e) *s*2, (f) *s*3 and (g) *s*AlO.

for zeolites and pumice, which is a natural amorphous aluminosilicate with composition similar to *s*0.17, the binding energies of all the elements, especially of silicon and oxygen, shift in the same direction [26]. This can be explained by assuming the presence of group units rather than elemental units in which the silica framework acts as the cation like unit and the alumina framework as anion [26–27]. As more Al–O units are inserted into a silica type framework, the binding energy of the Si (2*p*) peak progressively decreases to reflect the enhanced covalency induced into the Si–O bonds by the more ionic Al–O units [28]. The aluminum binding energy is less affected by the presence of silicon, its binding energy ranging between 74.6 eV from pure alumina to 75.2 eV for the highest Al/Si ratio oxide compound. Analogously to the aluminosilicate sodalite and zeolite Na-*A*, the increase of both Al 2*p* and Si 2*p*

Table 2
Al 2*p*, Si 2*p* and O 1*s* binding energies (eV) of the oxides with the FWHM in parentheses. For silicon and oxygen the relative percentage of each chemical species are reported

Samples	Al 2*p*	Si 2*p*	Relat. Si (%)	O 1*s*	Relat. O (%)
*s*AlO	74.7 (1.9)			531.1 (2.2)	
*s*3	74.7 (2.4)	100.0 (2.5)	23.6	531.3 (2.7)	80.8
		102.3 (2.5)	76.4	533.0 (2.7)	19.2
*s*2	74.6 (2.8)	99.5 (2.8)	18.9	531.1 (3.2)	
		102.2 (2.8)	81.1		
*s*1	75.1 (2.4)	100.6 (2.5)	9.0	531.8 (2.8)	
		102.8 (2.5)	91.0		
*s*0.3	75.3 (2.5)	100. 3 (2.6)	3.0	532.3 (2.8)	
		103.3 (2.6)	97.0		
*s*0.17	75.2 (2.6)	100.4 (2.6)	1.7	532.3 (2.8)	
		103.5 (2.6)	98.3		
*s*0	–	103.9 (2.3)	100	532.9 (2.4)	

binding energies with the decrease of the Al/Si ratio, is indicative of aluminate units located in tetrahedral environments, substituting some of the silicate units [28]. The nearly constant FWHMs obtained along the series of samples are a good indication of sample homogeneity. As it can be observed in Fig. 4, the Si 2*p* region presents an additional component at lower binding energy whose intensity increases with the increasing of alumina in the oxides. This feature lies at binding energy around 100 eV and is present in all samples, except pure silica, in different percentage. Its binding energy is typical for silicon in reduced state [29]. In Table 1 the bulk atomic ratio Al/Si, corresponding to the analytical sample composition, and the surface ratio as derived from XPS peak areas are also reported. The XPS data reported in column 3 refer to the total Si 2*p* intensity. In the same column, the values in parentheses represent the atomic ratios as obtained considering only the high energy component of the Si 2*p* peak. Bulk ratios slightly differ from the XPS ratios calculated with the total Si 2*p* areas. Contrary to XPS results on similar oxides, showing quite large discrepancy between the bulk and the surface composition, here the deviation is not very pronounced, and if we use only the silicon component at high binding energy, (see values in parentheses) the Al/Si ratio becomes close to the nominal [30]. In order to verify that the component at ca. 100 eV is indeed a surface species with a lower oxidation state due to surface distortion phenomena, angular variation measurements were carried out. If the Si reduced component was a surface species, its XPS intensity relative to the intensity of the oxidized species would increase with the increasing of the surface sensitivity. The study was made on the selected sample, *s*2. By decreasing the take off angle, considered with respect to the sample surface, therefore enhancing the surface sensitivity, a small but continuous increase of the Si $2p_{red}$ component relative to Si $2p_{ox}$ component

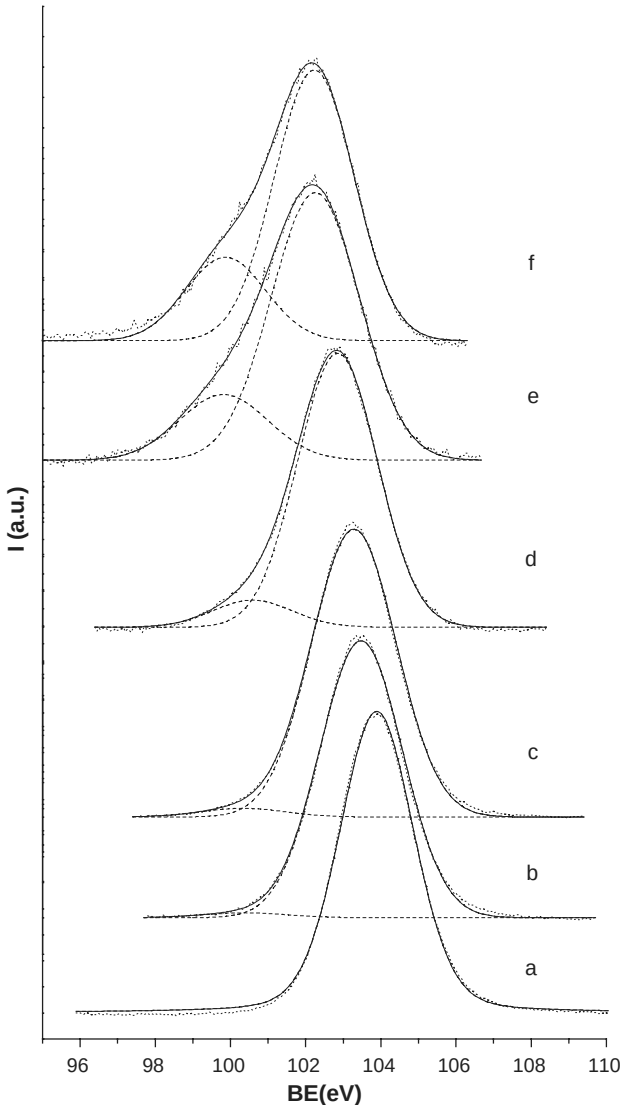

Fig. 4. Si 2*p* spectra of the oxides. (a) *s*0, (b) *s*0.17, (c) *s*0.3, (d) *s*1, (e) *s*2, and (f) *s*3. Dotted line: experimental data; solid line: fitted data; dashed line: fitted components.

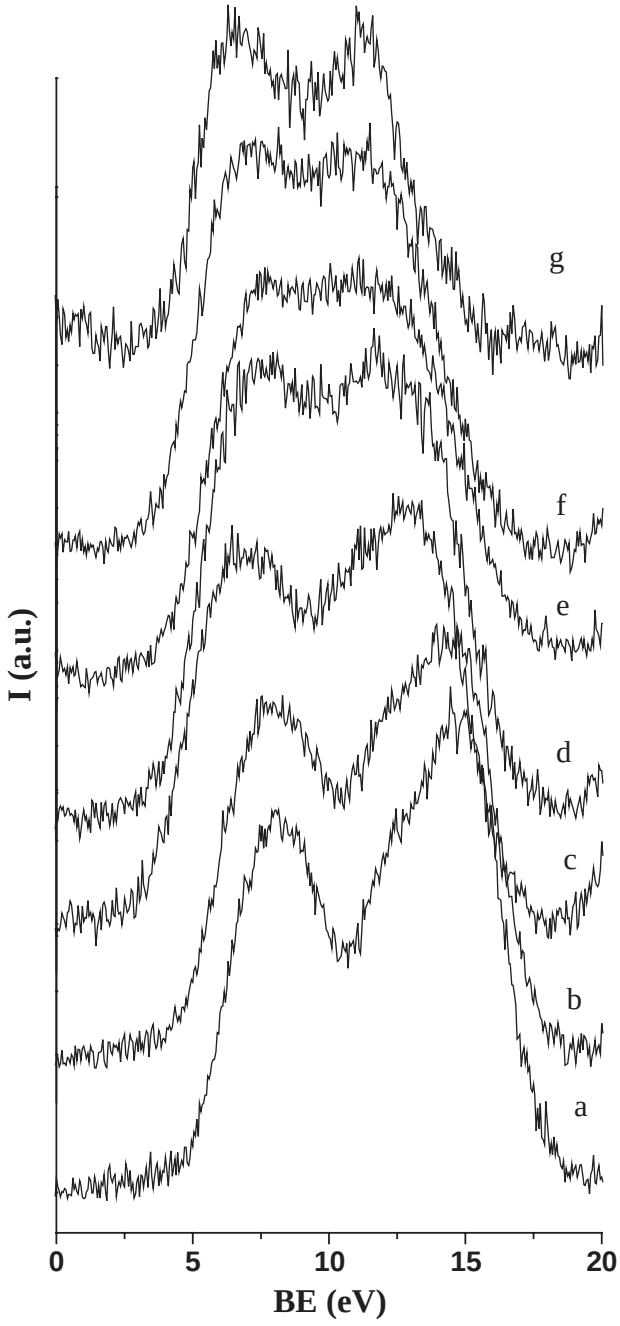

Fig. 5. Valence region of the oxides (a) *s*0, (b) *s*0.17, (c) *s*0.3, (d) *s*1, (e) *s*2, and (f) *s*3, (g) *s*AlO.

was observed. At the same time a decrease of the total Al 2*p* over Si 2*p* intensity ratio was also obtained. It can be concluded that, as also described in the literature for zeolites and other aluminosilicate a surface layer enriched in Si is formed [26,29].

The X-ray induced valence spectra of the alumina-silica oxides were also studied in the range 0–20 eV, and the relative spectra are shown in Fig. 5. The valence region changes with the relative percentage of the two oxides. The spectrum of pure silica (Fig. 5a) is rather broad (ca. 15 eV) and is divided into two substructures. The one centered at 8.1 eV is mainly due to O 2*p* non-bonding orbitals. The second substructure is quite broad and is divided into two sub-bands. One centered at 12.1 eV and due to bonding orbitals formed from O 2*p* and Si 3*p* and the other one at 14.9 eV due to bonding orbitals formed from O 2*p* and Si 3*s* [31]. The gulf between the two substructures is the bonding "barrier" and is a measure of the covalent character; the deeper is the gap the greater is the covalency. The spectrum of pure alumina is narrower than the silica one (ca. 9 eV) and again two sub-bands are observed; one centered at 6.6 eV due to the non-bonding O 2*p* orbitals and the other centered at 11 eV due to the bonding orbitals (O 2*p* and Al 2*p* or Al 2*s*). The gap between these two bands is rather shallow, indicating that alumina has less covalent bonding stabilization than silica with a larger degree of

ionicity [31]. The spectra of the low Al/Si ratio compounds are different from the corresponding spectra of zeolite with similar composition which are characterized by three different regions, they rather resemble the valence band of the amorphous natural pumice [27,31]. The shape of the band remains similar to the pure silica band in the mixed oxide with low Al/Si atomic ratio (up to the *s*0.3 sample) even though there is a downwards binding energy shift and a modification of the relative intensities of the two main substructures. These changes are in accord with the structure of silica slightly perturbed by aluminate ions. By increasing the alumina content the valence spectra resemble more closely the alumina one. The peak due to the non-bonding O 2*p* orbital moves down to 6.6 eV and the peak due to the bonding orbitals move to 11 eV. Moreover, the relative intensity of the two substructures inverts, and the gap becomes shallow.

3. Conclusion

To summarize, the synthesis sol–gel adopted in this study afforded the preparation of mixed silica-alumina oxides. The mixed oxides exhibited amorphous diffractogram, differently from the pure alumina sample characterized by the γ-Al_2O_3 phase. The lack of crystallinity even in the alumina rich samples was an indication of good molecular mixing. As shown by the IR spectra of adsorbed pyridine on three selected samples, Lewis acid sites of similar strength are present on the surface of the mixed oxides independently on the Al/Si atomic ratio. On the contrary, the Brønsted acid sites are formed essentially in the samples with higher percentage of silica. The region of the hydroxyl groups is characterized by an asymmetric band likely due to terminal silanol and bridging hydroxyl groups. From the quantitative XPS analyses, Al/Si atomic ratios in good agreement with the overall bulk ratios were obtained. A slight surface segregation of a species containing silicon in a reduced electronic state was also found. Such surface species was not detected on pure silica and therefore it seemed to be induced by the presence of alumina. Also indicative of good molecular mixing was the gradual variation of the structure of the valence spectra of the oxides, from the pure silica spectrum, characterized by a deep gap between two substructures, indicative of covalent Si–O bonding, to the pure alumina spectrum characterized by shallower gap, typical of larger degree of ionicity of the Al–O bond.

References

[1] H. Topsøe, B.S. Clausen, F.E. Massoth, in: J.R. Anderson, M. Boudart (Eds.), Hydrotreating Catalysis, Springer, Berlin, 1996.
[2] R. Voyatiz, J.B. Moffat, J. Catal. 142 (1993) 45.
[3] M. Breysse, J.L. Portefaix, M. Vrinat, Catal. Today 10 (1991) 489.
[4] J.B. Miller, I.E. Ko, Catal. Today 35 (1997) 269.
[5] K. Shibata, T. Kiyoura, J. Kitagawa, T. Sumiyoshi, K. Tanabe, Bull. Chem. Soc. Jpn. 46 (1973) 2985.
[6] K. Tanabe, T. Sumiyoshi, K. Shibata, T. Kiyoura, J. Kitagawa, Bull. Chem Soc. Jpn. 47 (5) (1974) 1064.
[7] R.G. Lelived, T.G. Ros, A.J. van Dillen, J.W. Geus, D.C. Koningsberger, J. Catal. 185 (1999) 513.
[8] J. Livage, M. Henry, C. Sanchez, Prog. Solid State Chem. 18 (1988) 259.
[9] C. Sârbu, B. Delmon, Appl. Catal. A 185 (1999) 85.
[10] A.M. Venezia, F. Raimondi, V. La Parola, G. Deganello, J. Catal. 194 (2000) 393.
[11] R. Navarro, B. Pawelec, J.L.G. Fierro, P.T. Vasudevan, Recent. Res. Dev. Catal. (1996) 1.
[12] A.M Venezia, V. La Parola, G. Deganello, GIC 2000, 1–5 Ottobre 2000, Ravello, Italia.
[13] A.M. Venezia, V. La Parola, G. Deganello, D. Cauzzi, G. Leonardi, G. Predieri, Appl. Catal. A 229 (2002) 261.
[14] S. Subramanian, J.S. Noh, J.A. Schwarz, J. Catal. 114 (1988) 433.
[15] S.J. Gregg, K.S. Sing, Adsorption Surface Area and Porosity, 2nd Edition, Academic Press, San Diego, 1982.
[16] D.A. Shirley, Phys. Rev. B 5 (1972) 4709.
[17] P.M.A. Sherwood, in: D. Briggs, M.P. Seah (Eds.), Practical Surface Analysis, Wiley, New York, 1990, p. 181.
[18] J.P. Brunelle, Pure Appl. Chem. 50 (1978) 1211.
[19] G. Busca, Catal. Today 41 (1998) 191.
[20] B.A. Morrow, I.A. Cody, J. Phys. Chem. 80 (1976) 1998.
[21] H. Knozinger, Adv. Catal. 25 (1976) 184.
[22] T.B. Beebe, P. Gelin, J.T. Yates, Surf. Sci. 148 (1984) 526.
[23] M. Trombetta, G. Busca, S. Rossini, V. Piccoli, U. Corsaro, A. Guercio, R. Catani, R.J. Willey, J. Catal. 179 (1998) 581.
[24] T.J. Bandosz, C. Lin, J.A. Ritter, J. Colloid Interface Sci. 198 (1998) 347.
[25] M. Schraml-Marth, K.L. Walther, A. Wokaun, B.E. Handy, A. Baiker, J. Non-Cryst. Solids 143 (1992) 1.
[26] T. Barr, M.A. Lishka, J. Am. Chem. Soc. 108 (1986) 3178.
[27] A.M. Venezia, M.A. Floriano, G. Deganello, A. Rossi, Surf. Interface Anal. 18 (1992) 532.
[28] B. Herreros, H. He, T.L. Barr, J. Klinowski, J. Phys. Chem 98 (1994) 1302.
[29] T.L. Barr, Appl. Surf. Sci. 15 (1983) 1.
[30] W. Daniell, U. Schubert, R. Glöckler, A. Meyer, K. Noweck, H. Knözinger, Appl. Catal. A General 196 (2000) 247.
[31] T.L. Barr, L.M. Chen, M. Mohsenian, M.A. Lishka, J. Am. Chem. Soc. 110 (1988) 7962.

• Cerâmica 45 (291) • Feb 1999 • https://doi.org/10.1590/S0366-69131999000100007 COPY

Aluminosilicates compacts by alkoxide route: influence of Ba addition

Compactos de aluminosilicatos pela rota dos alcóxidos: influência da adição de bário

Abstracts

The sol-gel route was employed to obtain three different powders with the stoichiometric composition corresponding to mullite (3 Al2O3.2SiO2): (i) commercial alumina and silica from sol-gel, (ii) alumina and silica by alkoxide partial hydrolysis, (iii) alumina and silica by alkoxide simultaneous hydrolysis. Tetraethylorthosilicate (TEOS) and aluminium tri-sec-butoxide were used as alkoxide precursor. Moreover, 5 wt% of barium, incorporated to precursor solutions as Ba-acetilacetonate, was used as additive to study its influence on densification and mullite phase formation. The precursor powders were pressed uniaxially to form green compacts, after that all samples were heated to 1350 °C for 2 hours to obtain densified pellets. X-ray diffration patterns of powders, obtained by milling of sintering compacts, showed important differences. In barium doped samples a higher grade of densification and a greater glassy phase formation were observed.

sol-gel; barium; alkoxides; aluminosilicates

O método sol-gel foi usado para obter pós com 3 composições estequiométricas correspondente a mulita (3 Al2O3.2SiO2): (i) alumina comercial e sílica por sol-gel, (ii) alumina e sílica por hidrólise parcial de alcóxido, (iii) alumina e sílica por hidrólise simultânea de alcóxido. Tetroetiloctosiliceto (teos) e tri-sec-butóxido de alumínio foram usados como precursores alcóxidos. Além disso, 5% em peso de bário, adicionado nas soluções precursoras como acetilacetonato de bário foi usado como aditivo para estudar sua influência na densificação e formação da fase mulita. Os pós precursores foram prensados uniaxialmente para formar compactos a verde, e posterior aquecimento a 1350°C por 2 h para obter corpos densificados. A difração raios X dos pós, preparados por moagem dos compactos sinterizados, mostrou diferenças importantes. Foram observadas maior densificação e formação de fase vítrea nas amostras dopadas com bário.</I>

sol-gel; bário; alcóxidos; aluminosilicatos

Aluminosilicates compacts by alkoxide route: influence of Ba addition

(Compactos de aluminosilicatos pela rota dos alcóxidos: influência da adição de bário)

N. E. Quaranta, E. R. Benavidez

Universidad Tecnológica Nacional - Facultad Regional San Nicolás

Colón 332 - (2900) San Nicolás - Argentina

e-mail: *nancyutn@cablenet.com.ar*

Abstract

The sol-gel route was employed to obtain three different powders with the stoichiometric composition corresponding to mullite (3 $Al_2O_3.2SiO_2$): (i) commercial alumina and silica from sol-gel, (ii) alumina and silica by alkoxide partial hydrolysis, (iii) alumina and silica by alkoxide simultaneous hydrolysis. Tetraethylorthosilicate (TEOS) and aluminium tri-sec-butoxide were used as alkoxide precursor. Moreover, 5 wt% of barium, incorporated to precursor solutions as Ba-acetilacetonate, was used as additive to study its influence on densification and mullite phase formation. The precursor powders were pressed uniaxially to form green compacts, after that all samples were heated to 1350 °C for 2 hours to obtain densified pellets. X-ray diffration patterns of powders, obtained by milling of sintering compacts, showed important differences. In barium doped samples a higher grade of densification and a greater glassy phase formation were observed.

Keywords: sol-gel, barium, alkoxides, aluminosilicates.

Resumo

O método sol-gel foi usado para obter pós com 3 composições estequiométricas correspondente a mulita (3 $Al_2O_3.2SiO_2$): (i) alumina comercial e sílica por sol-gel, (ii) alumina e sílica por hidrólise parcial de alcóxido, (iii) alumina e sílica por hidrólise simultânea de alcóxido. Tetroetiloctosiliceto (teos) e tri-sec-butóxido de alumínio foram usados como precursores alcóxidos. Além disso, 5% em peso de bário, adicionado nas soluções precursoras como acetilacetonato de bário foi usado como aditivo para estudar sua influência na densificação e formação da fase mulita. Os pós precursores foram prensados uniaxialmente para formar compactos a verde, e posterior aquecimento a 1350°C por 2 h para obter corpos densificados. A difração raios X dos pós, preparados por moagem dos compactos sinterizados, mostrou diferenças importantes. Foram observadas maior densificação e formação de fase vítrea nas amostras dopadas com bário.

Palavras-chave: sol-gel, bário, alcóxidos, aluminosilicatos.

INTRODUCTION

Mullite is the stable phase of aluminosilicate system at high temperature when the solid state reaction between Al_2O_3 and SiO_2 takes place. Properties of mullite such as low thermal expansion, low dielectric constant and high creep and mechanical resistance have identified mullite as a good candidate to be applied in electronic and in high temperature structural applications [1]. In view of the technological

importance of mullite in the field of ceramics, the synthesis of this material has been extensively investigated [2]. The synthesis reaction is modified by some factors such as: particle size distribution of precursor materials, mixing conditions, thermal treatment, Al/Si ratio, etc [3].

The temperature of mullite formation (mullitization) can be substantially decreased using finer powders of alumina and silica in an intimate mixing [4]. By this, it is very important to control synthesis conditions to obtain alumina-silica mixing with these properties. The size of particles in intimate contact affects the mullite formation temperature. Thus, temperatures above 1600

°C are necessary to obtain mullite when the particle size distribution is greater than one micron. Colloidal methods produce powders with particle size about 1 micron, in this case the reaction temperature is reduced to the 1300-1450 °C range [5]. Lower reaction temperatures (near 1000 °C) can be obtained when molecular level of mixing is achieved [6, 7]. This is the case corresponding to materials produced by sol-gel method [8, 9].

Very high purity and homogeneity in the precursor materials and a lower process temperature incorporated into sol-gel technique are advantageous characteristics compared to the conventional methods. Also by this method is possible to produce powder with high surface area which include very fine particles. The most important characteristic is to control material properties during the earliest stages of powder production. This introduces the concept of molecular manipulation [10].

In the present work, the sol-gel synthesis method was used to obtain materials with mullite composition, with and without barium addition. This addition was selected to study its influence on the densification and mullitization behavior of the samples.

MATERIALS AND METHOD

Samples preparation

Sample M1:

it was prepared from commercial alumina (Aldrich, 99.8%) with particle size < 10 mm, and silica obtained by alkoxide route using TEOS (Aldrich, 98%). First, alumina was suspended in TEOS/ethanol solution, then silica was synthesized by hydrolysis process. The hydrolysis taked place adding distilled water to a 0.02 mol/min rate under continuos stirring. The final molar ratio H

$_2$O:TEOS:EtOH = 4:1:1 was established in this experiment and ammonium hydroxide (NH

$_4$OH) was added to alkalize the solution at pH = 8. The experiment temperature was kept constant at 45 ° C. After 24 hours of reaction, the floating liquid was extracted and the sample was dried at 60 ° C.

Sample M2: it was obtained under similar conditions that M1, but alumina precursor was aluminum tri-sec-butoxide (Aldrich, 97). In this case, the partial hydrolysis method was employed [11]: Si-alkoxide was partially hydrolyzed for 2 h under the same conditions and proportions than M1, after that Al-alkoxide dissolved in ethanol, was added to Si solution.

Sample M3: similar conditions than M2 were established, but a different process step was employed in this preparation: simultaneous hydrolysis replaced the partial hydrolysis of Al and Si alkoxides.

Samples M1Ba, M2Ba, M3Ba: these materials were obtained similarly to M1, M2 and M3, respectively, adding barium acetilacetonate hydrate (Aldrich) to initial solutions. In all cases, the addition was fixed at 5 wt% Ba.

The powders obtained by different ways were compacted to disks 35.6 mm in diameter by uniaxial pressing. These compacts were heated to sintering temperature 1350

°C for 2 hours. Then they were cut, mounted and polished to allow for microscopy observation and microhardness characterization. The sintering temperature was established taking into account previous results [12].

Characterization of powders and compacts

All samples were characterized by the following methods:

(i) **Microscopy analysis**: microstructures of the polished sintered samples were observed by a Zeiss microscope with a Philips video camera.

(ii) **Specific surface area**: initial powders areas were determinated by BET method using N

2 gas with an Accusorb Micromeritics equipment.

(iii) **X-ray diffraction**: XRD patterns of sintered powders were obtained with Philips PW 1390 diffractometer, using CuK

a radiation and Ni filter. The operation conditions were 40 kV, 20 mA and scanning rate of 1°/min.

(iv) **Vickers microhardness**: these analyses were made with a Vickers identer in a HMW-2000 Shimadzu equipment at load of 300 g applied during 10 seconds on the polished surface of the sintered body.

(v) **Density determination**: bulk densities after sintering were measured by the Archimedes method using distilled water.

RESULTS AND DISCUSSION

Samples obtained by different ways showed a higher densification grade when barium was added, as it is observed in the density and radial shrinkage values shown in Table I. This behavior can be attributed to better initial properties corresponding to these samples, since it can be observed in the powder materials produced by the same way, the specific surface area was increased by Ba addition.

The low radial shrinkage corresponding to M1 and M1Ba samples, can be explained taking into account that a-alumina was employed in their preparation. In the other samples g-alumina are obtained in the precursor materials and transformed to a-phase by heating. This structural change is accompanied by an important volume contraction. The shrinkage is higher in samples with Ba, because a liquid phase appears at lower temperature than Al_2O_3-SiO_2system, promoting the densification grade of compacts. A greater glassy phase in all compacts with barium, compared to similar compacts without it, can be observed by optical microscopy.

These observations also explain microhardness results, that show lower values for samples containing barium. In Fig. 1 two photographs corresponding to M3 and M3Ba sintered compacts are shown; a higher sintering grade and a higher amount of glassy phase in M3Ba are observed.

Observing samples without Ba, the one obtained by partial hydrolysis (M2) presents the largest specific surface area, which is related to higher shrinkage and density.

terns as it is shown in Fig. 2. In M1 and M1Ba powders peaks corresponding to a-Al_2O_3, but no ected, indicating that silica is in amorphous phase and the mullite formation temperature is (1350 °C). Moreover, in M1Ba sample the $BaAl_2Si_2O_8$ phase is observed.

2

In the other samples are detected mullite and high intensity peaks of cristobalite but no peaks corresponding to a-Al_2O_3. This can be due to the formation of a Al_2O_3-rich mullite phase leaving free silica which it is stabilized in cristobalite structure. Similar behavior was already reported. [13] who founded a fast growth of cristobalite phase at 1350 ° C is found in samples with lower Al_2O_3 amount than the corresponding to mullite composition.

An important presence of cristobalite is observed in samples containing Ba. This fact contributes to obtain more densified compacts due to the volume contraction that takes place during amorphous silica to cristobalite transformation.

CONCLUSIONS

The sol-gel was used to obtain aluminosilicate powder samples with mullite composition. The different ways to obtain these samples and the influence of the barium addition (5 wt%) were studied. Some properties of these powders and corresponding sintered compacts were examinated.

1 - Samples obtained from commercial Al_2O_3 and sol-gel SiO_2 do not present mullite phase at the work temperature (1350 °C). The presence of barium has no influence on the compact densities and it is only observed like a low amount of $BaAl_2Si_2O_8$ phase.

2 - Partial hydrolysis as well as simultaneous hydrolysis of metal alkoxides produce SiO_2-Al_2O_3 mixture which at 1350 °C from mullite. In all cases, with and without barium addition, the cristobalite phase is observed. Barium addition favours cristobalite phase formation and contributes to obtain more dense ceramic compacts.

ACKNOWLEDGEMENTS

Dra. Quaranta, CICPBA researcher, gratefully acknowledges to this Commission for the financial support of the present work.

(Rec. 11/98, Ac. 01/99)

[1] S. Somiya, Y. Hirata, Am. Ceram. Soc. Bull. **70**, 10 (1991) 1624.

[2] K. Okada, N. Otsuka, S. Somiya, Am. Ceram. Soc. Bull. **70**, 10 (1991) 1633.

[3] S. Somiya, R. F. Davis, J. A. Pask, Ceramic Transactions, "Mullite and mullite matrix composites" **6** (1990), The American Ceramic Society, Inc.

[4] M. D. Sacks, H. Lee, J. A. Pask, " Mullite and mullite matrix composites", Ed. S. Somiya, R. Davis, J. Pask, Ceramic Transactions **6** (1990) 167.

[5] M. G. Ismail, Z. Nakai, S. Somiya, J. Am. Ceram. Soc. **70**, 1 (1987) C-7.

[6] J. Ossaka, Nature **91** (1961) 1000.

[7] T. D. McGee, D. Wirkus, Am. Ceram. Soc. Bull. **51**, 7 (1972) 577.

[8] S. Kansaki, H. Tabata, T. Kumazawa, S. Ohta, J. Am. Ceram. Soc. **68**, 1 (1985) C-6.

[9] B. Yoldas, D. Partlow, J. Mat. Sci. **23** (1988) 1895.

[10] L. Hench, J. West, Chem. Rev. **90** (1990) 33.

[11] H. Suzuki, Y. Tomokiyo, Y. Sumuya, H. Saito, J. Ceram. Soc. Japan Int. **96** (1988) 67.

[12] M. Caligaris, N. Quaranta, R. Caligaris, Key Engineering Materials **132-136**, (1997) 888.

[13] S. Kanzaki, M. Ohashi, H. Tabata, T.Kurihara, S. Iwai, S. Wakabayashi, " Mullite and mullite matrix composites", Ed. S. Somiya, R. Davis, J. Pask, Ceramic Transactions **6** (1990) 389.

Publication Dates

Publication in this collection
01 June 2000

Date of issue
Feb 1999

History

Accepted
Feb 1999

Received
Nov 1998